Available online at www.sciencedirect.com
SCIENCE DIRECT
Magnetic Resonance Imaging 23 (2005) 789–794
MAGNETIC RESONANCE IMAGING

MR safety and compatibility of a noninvasively expandable total-joint endoprosthesis☆

Robert J. Ogg[a,f,*], C. Brian McDaniel[d], Donald Wallace[a], Pierre Pitot[g], Michael D. Neel[c], Sue C. Kaste[a,b,e]

[a]Department of Radiological Sciences, St. Jude Children's Research Hospital, Memphis, TN 38105-2794, USA
[b]Department of Hemetology-Oncology, St. Jude Children's Research Hospital, Memphis, TN 38105-2794, USA
[c]Department of Surgery, St. Jude Children's Research Hospital, Memphis, TN 38105-2794, USA
[d]Wright Medical Technology, Arlington, TN 38002, USA
[e]Department of Radiology, College of Medicine, University of Tennessee Health Science Center, Memphis, TN 38163, USA
[f]Department of Biomedical Engineering, College of Health Science Engineering, University of Tennessee Health Science Center, Memphis, TN 38163, USA
[g]ID Partner, 38920 Crolles, France

Received 30 May 2005; accepted 16 June 2005

Abstract

A noninvasively expandable total-joint endoprosthesis is now available for pediatric patients; the prosthesis can be lengthened by external application of a magnetic field. We investigated the risks of unintentional heating or lengthening of the prosthesis during MR imaging and evaluated the effect of the device on the diagnostic efficacy of MR imaging of surrounding tissues. We performed MR imaging at 1.5 T by using standard pulse sequences and pulse sequences with high-gradient and high-radiofrequency duty cycle. MR imaging caused no measurable change in prosthesis length, and the temperature of the prosthesis increased by less than 1°C during repeated 14-min exposures. Despite significant signal loss and image distortion around the prosthetic joint, clinically useful images were obtained as close as 12 cm from the ends of the prosthetic stems, measured toward the body of the device. Thus, the prosthesis can be safely exposed to MR imaging pulse sequences at 1.5 T, and the visualization of some tissue surrounding the device is clinically useful.

Keywords: MR safety; MR compatibility; Prosthesis; Pediatric; Osteosarcoma

1. Introduction

Osteosarcoma is the most common malignant tumor of bone in children, and more than one third of cases occur in children younger than 10 years [1]. Osteosarcoma frequently involves the metaphysis of the distal femur or proximal tibia [1], and local control often necessitates resection of the involved physis. The orthopedic oncologist faces unique challenges in limb-salvage surgery for pediatric patients, because the continued normal growth of the contralateral lower extremity results in significant disparity in the length of the two limbs at skeletal maturity. In addition, prosthetic reconstruction can compromise bone growth in the affected limb by ablating the growth plate on the uninvolved side of the joint.

For skeletally immature children, the historic treatment-of-choice when malignant tumors of bone involved a major growth plate was amputation or rotationplasty [2–4]. Even for older children, standard limb salvage was avoided because of the potential for future significant difference in limb length [5]. Modular prosthetic devices [3,6–10] can be lengthened by replacing a midsection component; however, the lengthening of such devices requires multiple surgical procedures that frequently involved extensive surgical exposure and capsulotomy [6,8,11,12] and are often complicated by neurovascular injury, infection and postoperative stiffness [1,9,10,12,13].

The REPIPHYSIS (Wright Medical Technology, Arlington, TN), an endoprosthesis that is expanded noninvasively,

☆ Supported in part by Wright Medical Technology, by grants P30 CA-21765 and P01 CA-20180 from the National Institutes of Health and by the American Lebanese Syrian Associated Charities (ALSAC).

* Corresponding author. Department of Radiological Sciences, St. Jude Children's Research Hospital, Memphis, TN 38105-2794, USA. Tel.: +1 901 495 2758; fax: +1 901 495 3962.
E-mail address: robert.ogg@stjude.org (R.J. Ogg).

0730-725X/$ – see front matter © 2005 Elsevier Inc. All rights reserved.
doi:10.1016/j.mri.2005.06.008

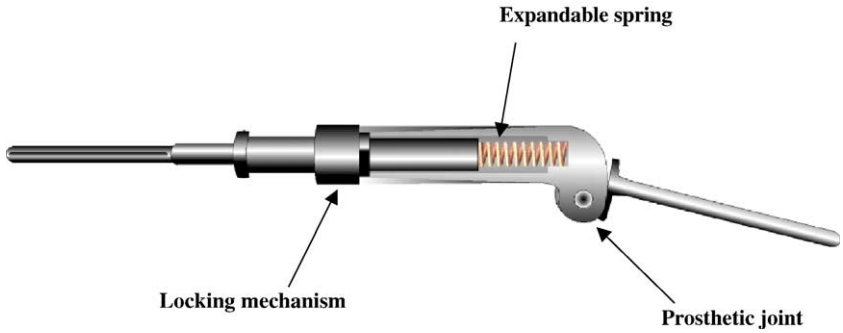

Fig. 1. Illustration of the REPYPHYSIS prosthesis.

is now in clinical use. This device provides an alternative surgical approach that improves patient satisfaction and limb function without compromising local control of primary bone tumors in a growing child [14]. The prosthesis is expanded by using a magnetic field to heat the locking mechanism by induction (Fig. 1); therefore, there is concern that clinical MR imaging procedures could cause unintentional lengthening or harmful heating of the device. Further, the primarily metal content of the prosthesis will interfere with MR imaging by causing significant metallic artifact and MR image degradation. We therefore investigated the risk of heating and accidental lengthening of the REPIPHYSIS device during MR imaging and evaluated the effect of the prosthesis on diagnostic MR imaging of surrounding tissues.

2. Methods and materials

2.1. Expansion of the prosthesis

The device is a modular endoprosthesis that is custom designed and custom manufactured for the individual patient's needs. It can be expanded without surgery to a length projected on the basis of three factors: the length of bone resected, the anticipated future growth of the contralateral extremity and the estimated disparity of limb length at skeletal maturity [5].

The expandable body of the device is a titanium tube that fits inside a polymeric tube (Fig. 1). At one end of the titanium tube, a locking mechanism penetrates the polymeric tube, locks the two parts together and allows prosthesis lengthening [5]. The exterior body of the prosthesis is made of polyether-ether ketone (PEEK) with a polyacetal tubular insert attached by a bolt. The closed extremity is connected to the titanium stem, which links the prosthesis to the residual bone.

Magnetic induction is used to noninvasively expand the prosthesis in the following manner: a coil is placed coaxially around the extremity such that the locking mechanism of the prosthesis is approximately at the center of the coil. The external coil couples energy to a heating ring within the locking mechanism. The heating ring is mounted with a ferrite rod at its center to concentrate magnetic flux through the ring. The relative permeability of the ferrite is approximately 1000 at the 90-kHz operating frequency, and the ferrite saturates at approximately 500 mT. The magnitude of the magnetic field applied during heating is 10 mT at the center of the coil. The induction heating field is applied for 15 to 30 s to raise the temperature of the heating ring to the melting point of the polyacetal insert (160°C). This allows the titanium tube under the force of a spring to slide out of the polymeric tube, thereby lengthening the prosthesis.

During a typical lengthening procedure, the temperature of the PEEK body increases to approximately 45°C, and that of the titanium tube increases less than 0.5°C. When the magnetic field is removed, the entire system cools and the polymeric tube solidifies to lock the interior titanium component in the new, longer position. The heat energy generated during lengthening is dissipated throughout the implant, the surface of which is sufficiently cooled by blood flow in the adjacent tissue to avoid significant heating of the surrounding local tissues. To protect muscles, blood vessels and nerves from excessive and potentially harmful

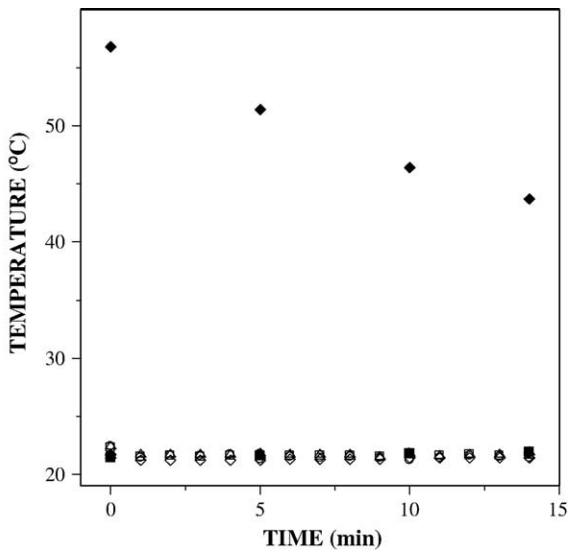

Fig. 2. MR imaging effect on the temperature of the prosthesis. Temperatures of four points on the device and a cup of hot water (filled diamonds) were measured every 1 or 5 min during the two 14-min exposures to MR pulse sequences.

stretching, the average increase in the length of the device per session is 8.5 mm (range, 5–20 mm) [5]. Therefore, serial lengthening procedures may be required until the patient completes longitudinal growth.

2.2. MR and radiographic imaging of the prosthesis

MR imaging was performed at 1.5 T with a Siemens Symphony MR scanner (Siemens, Erlangen, Germany) using typical pulse sequences and pulse sequences with a high-gradient and high-radiofrequency duty cycle. The maximum gradient amplitude was 30 mT/m with a maximum slew rate of 125 T/m per second. Three preclinical imaging experiments were performed. The first was designed to measure changes in the temperature of the prosthesis when time-varying (gradient and radiofrequency) magnetic fields were applied during MR imaging. The second was designed to evaluate the risk of MR-induced lengthening of the prosthesis. The third was designed to evaluate the effect of implant-induced signal loss and distortion on diagnostic MR images of the prosthesis and adjacent structures.

After evaluation of the preclinical data, we acquired MR images during a diagnostic evaluation of a 12-year-old patient with osteosarcoma who had been fitted with a REPYPHYSIS device.

2.2.1. MR-induced heating of the prosthesis

The prosthesis was supported in the MR unit on two rolls of bed sheets. Four bags of normal saline solution were placed beside the device to provide a signal for prescan adjustments of the MR system (e.g., frequency, transmitter amplitude). A Raytech Raynger ST Infrared Thermometer (model 4PD54) was used to sequentially measure the temperature of four equally spaced points on the PEEK body during MR imaging. This thermometer can measure temperatures as high as 398°C, and its accuracy is ±1% of the reading. We measured the temperature of a cup of hot water positioned at a similar distance from the thermometer but outside of the MR magnet to demonstrate the sensitivity of the thermometer to fluctuations in temperature.

The prosthesis was exposed to pulse sequences with gradient field (diffusion-weighted echo-planar, TR=184 ms, TE=105 ms, BW=1502 Hz/pixel, b=1000 s/mm^2) and radiofrequency field (turbo-spin-echo, echo train length=15, TR=1590 ms, TE=7.7 ms, BW=781 Hz/pixel, number of slices=1, slice thickness=2 mm, FOV=294 mm) duty cycle that is among the highest used in clinical MR imaging. These pulse sequences were used to maximize the potential for MR-induced heating of the prosthesis. Each high-duty cycle sequence was run continuously for 14 min. During the first run, we measured the temperature of the four points on the prosthesis every minute. During the second run, we measured the temperature of the prosthesis and that of a cup of hot water every 5 min.

2.2.2. MR-induced lengthening of the prosthesis

A cadaveric left leg with a total knee endoprosthesis in place was provided by Wright Medical Technology. Three sets of radiographs of the limb were obtained in the anterior–posterior (AP) and lateral views. All radiographs included a radio-opaque ruler with 1-cm marks. The first set was acquired before the limb was exposed to the MR-imaging system; the second set was acquired after MR imaging; and the third set was acquired after exposure to the

Fig. 3. Signal loss and distortion of MR images caused by the prosthesis. (A) T1-weighted image of the gel phantom. (B) T1-weighted image of a 12-year-old male patient with a prosthesis implanted in his left leg. The curving black lines are saturation bands that would appear as parallel vertical lines in the absence of the prosthesis. Note that the image is relatively intact near the ends of the shafts of the device.

Fig. 4. Adequate visualization of some soft tissue structures surrounding the prosthesis. MR images are shown of the lower extremities of a 12-year-old boy who underwent limb-sparing surgery with placement of a REPIPHYSIS prosthesis for osteosarcoma. Although artifact from the metallic prosthesis limits visualization of the epicenter of the joint, note the adequate visualization of the contralateral limb and useful visualization of some tissues in the vicinity of the ends of device. Coronal (A) and axial (B) noncontrast T1-weighted images demonstrate soft tissue edema without focal fluid collection (arrows). (C) Coronal STIR image through the same level shows soft tissue edema (arrows) without focal fluid collection. (D) Coronal contrast-enhanced T1-weighted MR image with fat saturation through the same level shows moderate soft tissue enhancement (arrow).

MR fields and after intentional, externally induced lengthening of the prosthesis.

After the baseline radiographs were evaluated, we performed MR imaging of the cadaveric specimen. Standard sequences typically used to image extremities were executed; these comprised T1 (TR=675, TE=7.1 ms, BW=390 Hz/pixel, echo-train length=7, averages=2, matrix=256×256, T2) and short tau inversion recovery (STIR) (TR=3095, TI=140 ms, TE=7.1 ms, BW=390 Hz/pixel, echo-train length=7, averages=1) sequences in coronal (FOV=480 mm, matrix=256×256, number of slices=15, slice thickness=4 mm, slice gap=1 mm) and axial (FOV=300 mm, matrix=256×256, number of slices=21, slice thickness=10 mm, slice gap=10 mm) planes. In addition, the specimen was exposed to the high-duty cycle pulse sequences described above.

We evaluated the signal-to-noise ratio and image homogeneity for the body coil and head coil by using standard quality assurance phantoms and test procedures provided by the manufacturer. The measurements were made with and without the cadaveric extremity containing the prosthesis in the magnet bore.

The noninvasive lengthening procedure was performed on the cadaveric specimen under fluoroscopic guidance to demonstrate that the device operated normally. The length of the spring was manually measured with calipers on hard copies of each set of radiographs. The maximum length of the spring was estimated from the apex of the flange to the most distal portion of the spring on each view.

2.2.3. Effects of the prosthesis on MR imaging of surrounding structures

To evaluate the extent to which the prosthesis interferes with MR imaging of surrounding structures, we embedded the device in an agar phantom that had MR relaxation parameters similar to those of muscle imaged at 1.5 T [15]. Briefly, agarose (2% w/v) was dissolved in saline supplemented with 0.2 mM copper sulfate (nominal T1=800 ms and T2=50 ms for the agar gel). The prosthesis was placed on small plastic supports within a plastic container. The agar solution was carefully poured to cover the prosthesis and minimize the entrapment of air.

MR imaging was performed with the standard body array coil, consisting of a two-channel anterior element and a four-channel posterior element. The system body coil was used for excitation. Imaging included T1-weighted and STIR sequences with the parameters listed above, except that the readout BW was maximized (780 Hz/pixel) to minimize prosthesis-induced image distortion [16]. To reveal the degree of spatial distortion caused by the prosthesis, we acquired images with and without saturation

bands applied through the phantom, perpendicular to the image plane, during each sequence. The images of the agarose phantom were then compared with images from a diagnostic study of a pediatric patient with osteosarcoma who had an implant. The patient was examined by using the same imaging protocol described above. The patient's legal guardian gave written informed consent for the imaging examination, and inclusion of the patient images in this report was approved by the St. Jude Children's Research Hospital Institutional Review Board.

3. Results and discussion

We found no evidence that magnetic forces acted on the prosthesis as it was handled near the MR magnet, nor did we find evidence that MR fields induce hazardous heating or lengthening of the prosthesis. The temperature of the prosthesis increased less than 1°C at all points measured during the 14 min of continuous exposure to MR pulse sequences with either high-gradient or high-radiofrequency duty cycle (Fig. 2). This temperature change is less than one eighth of the temperature increase that is typically induced in the implanted device during the lengthening procedure and poses no thermal risk to patient health [17]. Further, this increase was measured directly from a device that was not implanted. The MR-induced temperature increase of an implanted prosthesis would be even less, because blood circulation would quickly dissipate the heat. Therefore, the risk of inadvertent heating of the device during standard MR imaging is minimal.

Before MR imaging, the length of the spring within the prosthesis implanted in the cadaveric specimen was 1.0 cm, as determined on both the AP composite image and the AP view of the femur. After MR imaging, the length of the prosthesis was unchanged (data not shown). After the intentional lengthening procedure was completed, the spring measured 1.6 cm on the AP view. This degree of expansion was anticipated and demonstrated proper functioning of the device. Therefore, the risk of inadvertent lengthening of the prosthesis by standard MR imaging is minimal, and MR imaging does not impair the functioning of the lengthening mechanism of the prosthesis.

Two factors account for the lack of significant heating or inadvertent lengthening of the prosthesis during MR imaging: First, the power in the fluctuating gradient and radiofrequency fields is not sufficient. Second, the magnetic properties of the ferrite element in the induction heating system decrease coupling between the fluctuating MR fields and the heating ring in the prosthesis during MR imaging. The power delivered to the heating ring is proportional to the square of the induced electromotive force (emf) and inversely proportional to the resistance of the heating ring. The induced emf is proportional to the rate of change of the magnetic flux density (B) through the ring, which increases with the frequency (f) of the magnetic field fluctuations. The resistance in the heating ring increases as the square root of the frequency because of the skin effect [18]. Thus, heating of the ring varies as $B^2 f^{3/2}$.

For gradient fields, the flux density is about the same as that of the field applied during the lengthening procedure (~10 mT), but the frequency of the fluctuation of the gradient field is much lower. For a typical echo-planar acquisition, the fundamental frequency is approximately 1 kHz (i.e., 100 readout lines in 50 ms). This frequency is nearly two orders of magnitude lower than that of the magnetic field applied during the lengthening procedure (90 kHz), and the heating is negligible because of the $f^{3/2}$ dependence. For radiofrequency fields, the frequency is high, but the magnitude of the magnetic flux density (~10 μT) is approximately three orders of magnitude lower than that of the field applied during the lengthening procedure. Heating by the radiofrequency field is negligible because of the B^2 dependence.

The possibility of significant heating during MR imaging is reduced further by the magnetic properties of the ferrite component of the induction heating system. The ferrite is essential to achieve sufficient heating during intentional lengthening. The ferrite substantially increases the magnetic flux density within the heating ring (relative permeability ~1000), which increases the power coupled to the heating ring from the lengthening coil [19]. However, the ferrite saturates at field strength of approximately 0.5 T; therefore, the ferrite is saturated in the static field of the MR scanner (1.5 T). The magnitude of the fluctuations in the gradient and radiofrequency fields is insufficient to cause any oscillation of the ferrite magnetization, so the effective permeability of the ferrite during MR imaging is approximately 1. Therefore, even if the power in the fluctuating MR fields was comparable to that of the field applied during the lengthening procedure, the coupling to the heating ring would be negligible, because the ferrite is saturated. Also note that for radiofrequency magnetic fields the ferrite becomes lossy and dissipates magnetic flux. Therefore, the coupling of radiofrequency energy to the heating ring would be inefficient, even if the ferrite was not saturated by the static field.

The standard quality assurance phantom showed no degradation of standardized signal-to-noise ratio or image homogeneity measurements when placed in the magnet bore with the cadaveric leg containing the prosthesis. However, the metal components of the prosthesis did cause significant local distortion on MR images of the agar phantom (Fig. 3A) and on MR images of the patient's left lower extremity that contained the implant (Fig. 3B). Therefore, significant signal loss around the body of the prosthesis compromised the diagnostic evaluation of tissue in that region. In addition, there was substantial spatial distortion of images throughout most of the phantom (Fig. 3A). Despite these distortions around the body of the prosthesis, soft tissue around the shafts was adequately visualized within 12 cm of the ends of the prosthesis, measuring toward the joint (Fig. 4). Therefore, MR imaging should still be a valuable

diagnostic tool for patients who have undergone limb salvage and have an implant. MR imaging of an extremity that contains a prosthetic implant should be able to detect tumor recurrence, infection, edema (Fig. 4A–C) and contrast enhancement (Fig. 4D) in soft tissue around the stems at each end of the prosthesis.

Our findings demonstrate that this noninvasively expandable total-joint endoprosthesis can be safely exposed to MR scanners and imaging pulse sequences, at least in those systems that operate at 1.5 T. MR-induced lengthening of the prosthesis is unlikely in any MR system used for human imaging, because of safety limits on the power of applied fields as compared to the power required for intentional lengthening. Mechanical forces on the device and image distortion may be greater at higher static field strength. We conclude that there are no apparent contraindications to MR imaging at 1.5 T for patients who have undergone limb-sparing procedures and have an implanted REPYPHYSIS prosthesis.

Acknowledgment

The authors thank Caroline Phillips, RT(R)(MR), for prosthesis scanning and Angela McArthur for editing the manuscript.

References

[1] Simon MA, Springfield D, editors. Surgery for bone and soft-tissue tumors. Philadelphia (PA): Lippincott-Raven; 1998. p. 487–96.
[2] Akay M, Aslan N. Numerical and experimental stress analysis of a polymeric composite hip joint prosthesis. J Biomed Mater Res 1996;31:167–82.
[3] Baumgart R, Betz A, Schweiberer L. A fully implantable motorized intramedullary nail for limb lengthening and bone transport. Clin Orthop Relat Res 1997;343:135–43.
[4] Van Nes CP. Rotationplasty for congenital defects of the femur: making use of the ankle of the shortened limb to control the knee joint of a prosthesis. J Bone Joint Surg 1950;32B:12–6.
[5] Neel MD, Wilkins RM, Rao BN, Kelly CM. Early multicenter experience with a noninvasive expandable prosthesis. Clin Orthop Relat Res 2003;415:72–81.
[6] Eckardt JJ, Kabo JM, Kelley CM, et al. Expandable endoprosthesis reconstruction in skeletally immature patients with tumors. Clin Orthop Relat Res 2000;373:51–61.
[7] Eckardt JJ, Safran MR, Eilber FR, Rosen G, Kabo JM. Expandable endoprosthetic reconstruction of the skeletally immature after malignant bone tumor resection. Clin Orthop Relat Res 1993;297:188–202.
[8] Lewis MM. The use of an expandable and adjustable prosthesis in the treatment of childhood malignant bone tumors of the extremity. Cancer 1986;57:499–502.
[9] Schindler OS, Cannon SR, Briggs TWR, Blunn GW. Stanmore custom-made extendible distal femoral replacements. Clinical experience in children with primary malignant bone tumours. J Bone Joint Surg Br 1997;79:927–37.
[10] Schindler OS, Cannon SR, Briggs TW, et al. Use of extendable total femoral replacements in children with malignant bone tumors. Clin Orthop Relat Res 1998;357:157–70.
[11] Cool P, Davies M, Grimer RJ, Carter SR, Tillman RM. Growth in the lower limb following chemotherapy for a malignant primary bone tumour: a straight-line graph. Sarcoma 1997;1:75–8.
[12] Eckardt JJ, Eilber FR, Dorey FJ, Mirra JM. The UCLA experience in the limb salvage surgery for malignant tumors. Orthopedics 1985;8:612–21.
[13] Eckardt JJ, Eilber FR, Grant T, et al. Management of stage IIB osteosarcoma: experience of the University of California, Los Angeles. Cancer Treat Symp 1985;3:117–30.
[14] Wilkins RM, Soubeiran A. The Phenix expandable prosthesis: early American experience. Clin Orthop Relat Res 2001;382:51–8.
[15] Viano AM, Gronemeyer SA, Haliloglu M, Hoffer FA. Improved MR imaging for patients with metallic implants. Magn Reson Imaging 2000;18:287–95.
[16] Mitchell MD, Kundel HL, Axel L, Joseph PM. Agarose as a tissue equivalent phantom material for NMR imaging. Magn Reson Imaging 1986;4:263–6.
[17] Moritz AR, Henriques Jr FC. Studies on thermal injury: II. The relative importance of time and surface temperature in the causation of cutaneous burns. Am J Pathol 1947;23:695–720.
[18] Paris DT, Hurd FK. Basic electromagnetic theory. New York: McGraw-Hill; 1969.
[19] Feynman RP, Leighton RB, Sands M. The Feynman lectures on physics. Reading: Addison-Wesley; 1964.